Journal of Medicinal Chemistry

ARTICLE

pubs.acs.org/jmc

Recognition of Drug Degradation Products by Target Proteins: Isotetracycline Binding to Tet Repressor†

Gesa Volkers,‡ Lothar Petruschka,§ and Winfried Hinrichs*,‡

‡Department of Molecular Structural Biology, Institute for Biochemistry, University of Greifswald, Felix-Hausdorff-Strasse 4, D-17489 Greifswald, Germany

§Department of Genetics of Microorganisms, Interfaculty Institute for Genetics and Functional Genomics, University of Greifswald, Friedrich-Ludwig-Jahn-Strasse 15a, D-17489 Greifswald, Germany

ABSTRACT: Tetracycline antibiotics and their degradation products appear in medically treated tissues, food, soil, and manure sludge in the environment. In the context of protein interactions with various tetracyclines we performed crystal structure analyses of the tetracycline repressor in complex with weak or noninducing tetracycline derivatives. Isotetracyclines are degradation products of tetracyclines, which occur under physiological conditions. The typical framework of the antibiotic is irreversibly broken at the BC-ring connection, leading to a modified orientation of the AB to the new C*D ring fragments. The shape of the zwitterionic AB-ring fragment is unchanged and still binds to the TetR recognition site in a manner comparable to the intact antibiotic but without typical Mg^{2+} chelation. This work is an example that drug degradation products can still bind to specific targets and should be discussed in light of potential and critical side effects.

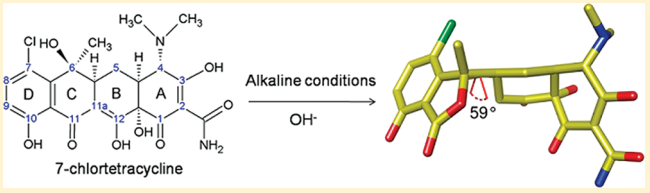

INTRODUCTION

The tetracycline repressor (TetR) regulates the efflux mechanism of tetracycline resistance in Gram-negative bacteria to inhibit prokaryotic ribosomal polypeptide elongation. Expression of the cytoplasmic membrane embedded efflux protein TetA is under tight control of TetR. The repressor induces expression of TetA upon binding of a tetracycline−magnesium chelate complex, $[MgTc]^+$. Tetracyclines (Tc) are only active antibiotics as chelate complexes which bind to the ribosome, the elongation factor *Tu*, and the efflux protein TetA and induce TetR.[1−5] The TetR/Tc system is known as a tight genetic switch and was further developed to control prokaryotic and eukaryotic gene expression in fermentation protocols, cell biological research, and gene therapy. In this context usage of chemically modified tetracyclines and TetR variants to create new specificities is well-known.[6] This is due to numerous hydrophilic and hydrophobic interactions of tetracycline in the binding tunnel of TetR, maintaining high affinity in the nanomolar range. Modifications of the hydrophilic part of the substitution pattern of the tetracycline framework (Figure 1A) lead to loss of antibiotic properties.[7]

Tetracyclines can be degraded enzymatically[8,9] but are also prone to undergo intramolecular rearrangements in aqueous solutions at acidic and basic pH conditions.[8,9] Under acidic conditions a reversible change in the C4 stereochemistry can lead to C4 β-epimers of tetracyclines,[10] which have been detected in muscle and organ tissues of animals.[11] The 4β-epimer of tetracycline possesses only 5% activity against *Klebsiella* compared to the 4α-epimer. This epimerization is inhibited by metal chelation and neighboring substituents at C2 and C5.[12]

Tetracyclines with a hydroxyl group in position 6 are irreversibly dehydrated to 5a,6-anhydrotetracyclines under strong acidic conditions and increased temperature.[13] Basic conditions degrade tetracyclines with a 6-hydroxy substituent to isotetracyclines (iso-TC),[14,15] e.g., iso-7-chlortetracycline (iso-CTC). The irreversible formation of iso-TCs was discovered shortly after tetracyclines were introduced as antibiotics. The reaction is induced by alkaline catalyzed cleavage of the C11−C11a bond by nucleophilic attack of the hydroxyl group in position 6 to C11, resulting in lactonization of the carbonyl group in position 11 (Figure 1A). The tetracene framework (rings labeled A−D) is modified to a phthalide, and the extended conjugated system at ring D with the former β-keto−enol moiety at atoms C11 and C12 is lost during the rearrangement process. Consequently, the typical chelation of a divalent metal ion becomes impossible by iso-TCs.[16] The complex formation is a prerequisite for antibiotic function, e.g., binding to the prokaryotic ribosomal target or induction of TetR.[17]

7-Chlortetracycline (aureomycin, CTC) is particularly vulnerable to isomerization when it is heated at pH 7.5, whereas tetracycline and oxytetracycline need pH > 9 to form isotetracycline and isooxytetracycline.[18] Isomerization causes an absorption shift to 300−380 nm, which can be only observed in alkaline pH range. Opening of ring C leads to isotetracyclines, resulting in vigorous decrease of antibiotic activity in vitro and complete loss of activity in vivo. Isotetracyclines do not inhibit the tetracycline/proton antiport protein (TetA) mediated uptake of tetracyclines

Received: March 22, 2011
Published: June 23, 2011

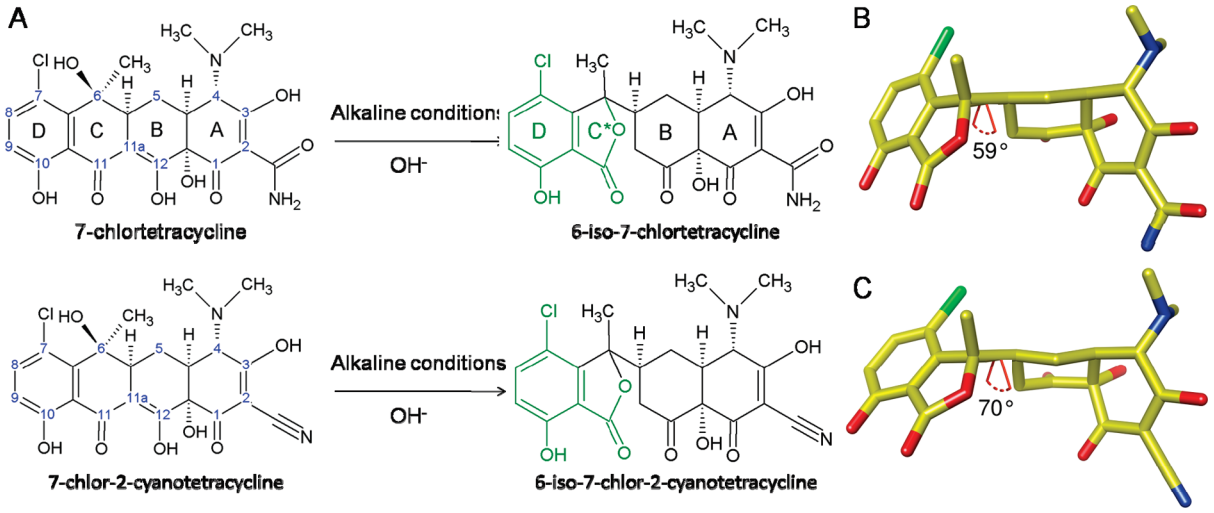

Figure 1. (A) Chemical structures of 7-chlortetracycline (CTC) and 7-chlor-2-cyanotetracycline (CNTC) that degrade under alkaline conditions to iso-7-chlortetracycline (iso-CTC) and iso-7-chlor-2-cyanotetracycline (iso-CNTC), respectively. In comparison to TetR(D)/$[MgCTC]^+$ binding the C*D ring moiety (green lines) is the only displaced part of both iso-TCs. (B) Structure of iso-CTC of the TetR(D)/iso-CTC complex. The formerly coplanar CD ring is rotated out of plane to ring B by 59°, which is possible because of free rotation of the C6−C5a bond. (C) In the case of the iso-CNTC complex the new C*D fragment is rotated out of plane to ring B by 70°.

into everted inner membrane vesicles from tetracycline resistant *E. coli*.[19] Growth of tetracycline sensitive and resistant soil bacteria is not inhibited by iso-CTC in the inhibitory concentration range of its precursor. The half maximal effective concentration of iso-CTC on aerobic sludge and soil bacteria is about 121-fold higher compared to CTC. The minimum inhibitory concentration of iso-CTC on *Pseudomonads* is 64-fold higher than that of CTC and reveals that formation of isotetracyclines coincides with the loss of antibiotic activity.[20]

High amounts of iso-CTC instead of its precursor were found in tissue like beef calf as degradation products after treatment with a medical relevant application rate of CTC.[21] Isoderivatives can be found in manure, and their precursors have been shown to be directly excreted to the soil by animals.[22] Recently, iso-CTC and 4-epi-iso-CTC have been identified as the principal metabolites of CTC in hen eggs whereas none of the precursor that was used to treat egg-laying chickens was found in eggs, so iso-TCs play a major role as metabolites of tetracyclines in the range pH 6.5−9.[23] Because of its higher solubility compared with its precursor CTC, iso-CTC is present in manure slurry, where it may have influence on the development of antibiotic-resistant soil bacteria. The compound 6-desmethyl-iso-CTC was found to be present in hens' plasma and egg yolk but not in egg white.[24] Altogether degradation processes of tetracyclines are inevitable.

Though iso-TCs do not show toxic effects on bacteria, it is not clear whether they influence resistance development, but since they are found as main degradation products in the environment, they should be regarded as potentially bioactive. The widespread use of tetracycline as a broad spectrum antibiotic together with its limited stability and the formation of degradation products suggest that the isoderivatives of tetracyclines play an important role in the environment. The influence of the tetracycline degradation products anhydrotetracycline, epitetracycline, and epianhydrotetracycline on the selection for tetracycline resistant or sensitive phenotypes of bacteria was demonstrated recently,[25] favoring selection of the sensitive phenotype. The mechanism of this process is complex, but comparable effects might be expected for iso-TCs.[26]

Iso-TCs are formed under physiological pH conditions. We demonstrate recognition of these degradation products by a specific protein target by crystal structure analyses. Examples are Tet repressor class D, TetR(D), in complex with both the isoforms of 7-chlortetracycline and 7-chlor-2-cyanotetracycline (CNTC) to a final resolution of 2.35 and 2.30 Å, respectively.

The bases to discuss iso-TC complexes of TetR(D) are several crystal structure analyses previously published (13 PDB entries) and reviewed in Saenger et al.[4] The quaternary structure of TetR(D) is a homodimer with a 2-fold rotation axis. Each polypeptide consists of 207 amino acid residues, which are folded into 10 α-helices with various turn connections (helices α1−α10 and symmetry related α1′−α10′). The N-terminal DNA-binding domains consist of a three-helix bundle with typical helix−turn−helix motifs for operator recognition. The orientation of the recognition helices determines the ability of TetR(D) to specifically bind to the DNA sequence of the palindromic operator *tet*O. The DNA-binding domains are linked to the globular regulatory core by helices α4 and α4′. Tetracycline−Mg^{2+} complexes, $[MgTc]^+$, bind in both symmetry related inducer binding tunnels of the regulatory core domain and trigger a cascade of conformational changes that abolish the high affinity of TetR to *tet*O. The allosteric mechanism starts with C-terminal changes of the α-helical conformation of the short helix α6 (residues 96−102). Residues His100 to Thr103 fold into a β-turn type II modifying the contact to α4 which changes the orientation of the DNA-binding domain in a pendulum-like motion. Thus, the conformation of the polypeptide segment determines the induced or not-induced state of TetR. This mechanism was proposed by comparison of crystal structure analyses of TetR(D) complexes with $[MgTc]^+$ (induced) and the *tet*O fragment (not induced).[27,28] Extended molecular dynamics studies provided evidence for the proposed mechanism.[29]

RESULTS AND DISCUSSION

Tet Repressor Structure. TetR(D) in complex with iso-TCs crystallized isomorphously to previously published structures.[27,28]

dx.doi.org/10.1021/jm200332e |*J. Med. Chem.* 2011, 54, 5108–5115

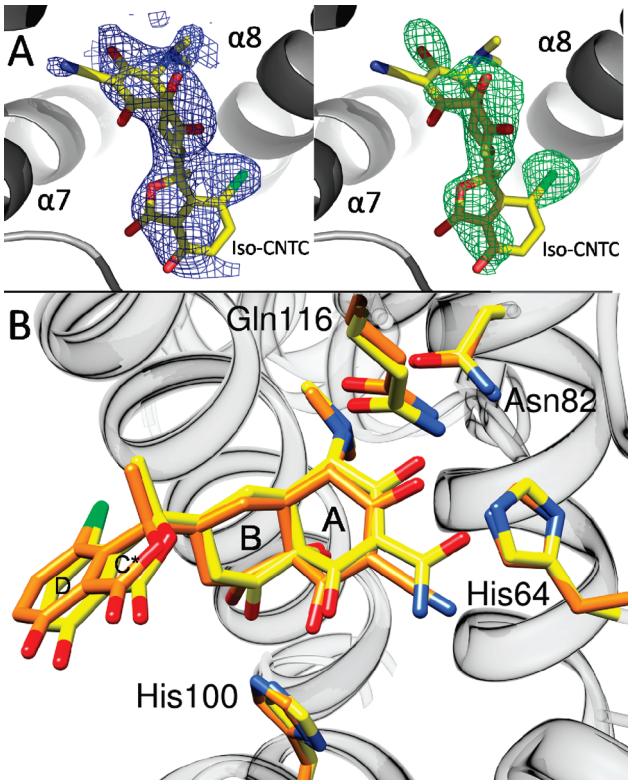

Figure 2. (A) Omit electron density maps of the iso-CNTC ligand in the TetR(D)/iso-CNTC structure: (left) $2F_o - F_c$ map at 1σ, blue; (right) $F_o - F_c$ map at 3.0σ, green. (B) Superposition of the TetR(D)/iso-CNTC (orange) and TetR(D)/iso-CTC (yellow) complexes.

The local dyad of the homodimer coincides with a crystallographic 2-fold axis. In both cocrystallized complexes of TetR(D) with iso-7-chlortetracycline (iso-CTC) and iso-7-chlor-2-cyanotetracycline (iso-CNTC) the modified drugs occupy the tetracycline binding site.

Isotetracycline Structure. TetR(D)/iso-TC complexes are the first examples that show the structures of iso-TC compounds by X-ray crystallography. The unambiguous identification of iso-TCs in the TetR binding pocket was possible during the initial stage of the refinement process before including any tetracyclines or isoforms into the structural models by observation of the $2F_o - F_c$ and $F_o - F_c$ electron density maps and comparison to other TetR(D)/Tc complexes (Figure 2A). Electron density for iso-CTC and iso-CNTC was visible, and the isotetracyclines were fitted into the electron density.

TetR Induction. TetR(D) in complex with iso-CNTC does not show the induced β-turn type II conformation of residues 100−103. Compared to the structure of TetR(D) crystallized with CTC (PDB code 2TCT[30]), the C_α-atom of Gly102 is shifted by 3.3 Å toward helix α4. Residues Leu101 and Gly102 are still part of helix α6 according to their main-chain torsion angles.

The iso-CNTC complex clearly adopts the not-induced conformation, whereas the situation of the iso-CTC complex remains unclear. In this complex the electron density of the critical β-turn (residues His100−Thr103) is fragmented and rather weak, making an unambiguous tracing of the polypeptide chain impossible. In other structures the section of electron density is very well-defined in both states, the induced and not-induced TetR(D). Here, the orientation of the peptide bond (peptide flip) of Leu101 to Gly102 cannot be interpreted unambiguously as induced or not-induced. Both possibilities refine to comparable quality parameters. Thus, TetR(D) in complex with iso-CTC is probably at the borderline of induction and we see an average of several intermediate steps of the allosteric transition of the α-helical conformation of C-terminal His100 to Gly102 of α6 to the β-turn 100−103. Superposition of TetR(D)/iso-CTC, TetR(D)/iso-CNTC, and the not-induced TetR(D) with the TetR(D)/$[MgCTC]^+$ complex using the rigid core (helices α8, α10, α8′, and α10′) as template demonstrates that the backbone of residues 100−106 and the N-terminus of α7 more likely adopt the induced state in the case of the TetR(D)/iso-CTC complex. The TetR(D)/iso-CNTC complex superposes better with the not-induced TetR(D) structure (Figure 3A).

Binding and Recognition of Isotetracyclines by the Tet Repressor. The overall structure and positioning of both iso-TCs in the TetR binding pocket are very similar (Figure 2B). The tetracycline framework is broken into two connected rigid pieces at the former C−C bond between C11 and C11a: the AB fragment and the phenolic D-ring with the attached coplanar γ-lactone as a new ring C*. The recognition of these substructures by TetR(D) can be discussed separately.

AB Fragment. The AB-ring fragment has the same shape as observed for tetracyclines in complex with proteins associated with antibiotic properties (TetR, EF-*Tu*). After insertion of tetracycline into the TetR binding tunnel, the initial recognition and binding rely on hydrogen bonds of substituents of the A ring to side chains of His64, Asn82, Phe86, and Gln116. The AB-ring fragment of the isoderivatives is in a very similar position as known for CTC in the TetR(D)/$[MgCTC]^+$ complex. In the iso-CTC complex we see exactly the same pattern of hydrogen bonds for the A-ring as known for tetracyclines (Figure 3B). The amide side chain of Asn82 interacts with the positively charged dimethylammonium group at position C4 and with the enolate O3 at position C3. The enolate additionally hydrogen-bonds with the imidazole of His64 and the side chain of Gln116. Side chains of His64 and Gln116 also form hydrogen bonds to the carbonyl oxygen of the carboxamide in position 2 of iso-CTC. The hydroxyl substituent at C12a is involved in an O−H···π interaction to the aromatic plane of Phe86, similar to the 2TCT complex and other TetR/Tc complexes. This protonation pattern of tetracyclines was verified by a quantum chemical approach.[31]

C*D Fragment. In comparison to the TetR/$[MgCTC]^+$ complex we see in both iso-TC complexes that only one-third of the former antibiotic molecule has changed the atom positions because of the isomerization. All displaced atoms belong to the phthalide moiety (see Figure 1A). The rings C* and D of the isoderivatives are still coplanar but are rotated at the single bond C5a−C6 against the B ring by 59° and 70° in the cases of iso-CTC and iso-CNTC, respectively (Figure 1B,C). The chlorine substituent at C7 of the aromatic D ring is shifted (about 6.3 Å) and rotated toward the side chain His139 and embedded in a more polar environment than in the custom binding mode of tetracyclines to TetR. Therefore, iso-TCs are clearly distinguished from tetracyclines in the observed electron-density omit maps (Figure 2A). In both iso-TC complexes the chlorine adopts the same position. The chlorine is enclosed in a polar environment formed by side chains of Ser135, Ser138, and His139, supporting recognition of these iso-TCs. A hydrophobic pocket for the aromatic D ring is maintained by side chains of Arg104

dx.doi.org/10.1021/jm200332e |*J. Med. Chem.* 2011, 54, 5108–5115

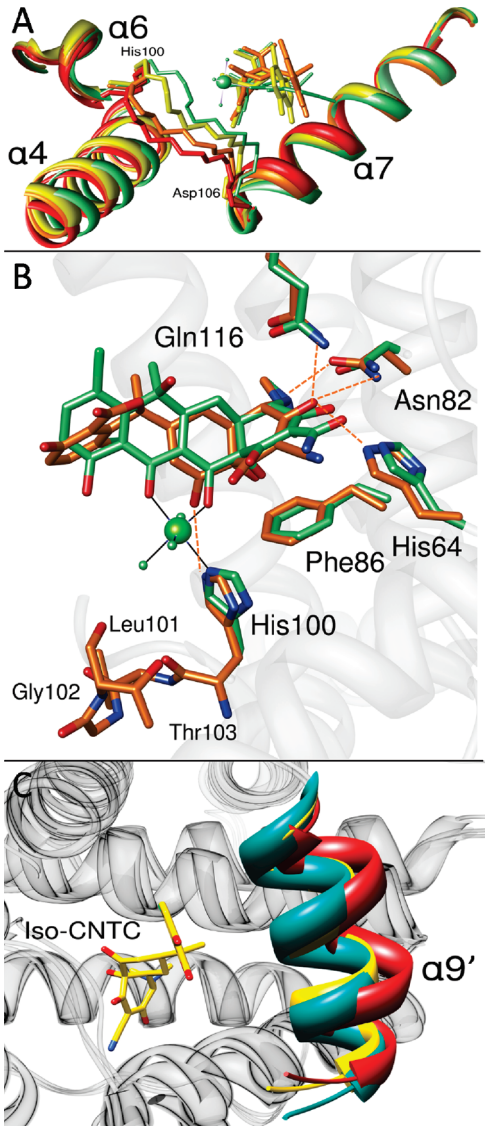

Figure 3. (A) Superposition of the not-induced TetR(D) structure (PDB entry 1A6I, red), the TetR(D)/iso-CNTC complex (orange), and the TetR(D)/iso-CTC complex (yellow) with the induced TetR(D)/[MgCTC]$^+$ complex (PDB entry 2TCT, green) shows that residues 100−106 of the TetR(D)/iso-CTC complex more likely adopt the induced conformation, whereas the TetR(D)/iso-CNTC complex is more similar to the not-induced conformation of TetR(D). (B) Superposition of the TetR(D)/iso-CNTC complex (orange) with the TetR(D)/[MgCTC]$^+$ complex (green, Mg^{2+} as large sphere, water ligands as spheres). The A-ring of iso-CNTC in the tetracycline binding site of TetR(D) hydrogen-bonds (dashed lines) with side chains of His64, Asn82, Gln116, His100, and Phe86. Residues 100−103 remain in the not-induced conformation. His100 hydrogen-bonds with the carbonyl O12 of iso-CNTC. (C) Superposition of the homodimeric structures of TetR(D)/iso-CNTC (yellow) with the TetR(D)/[MgCTC]$^+$ complex (cyan) and the not-induced TetR(D) structure without ligand (red). Only the ligand iso-CNTC is shown. The orientation of helix α9′ depends on the presence of a ligand. Helix α9′ adopts the same position in both the induced TetR(D)/[MgCTC]$^+$ and the not-induced TetR(D)/iso-CNTC complex because of hydrophobic interactions with the ligand.

and Pro105 together with the side chain of Met177′. The ester atom O6 and the methyl group C61 (both substituents of the former C6 of CTC) are in almost the same position compared to the CTC complex. The hydrophobic side chain of Val113 points toward oxygen O6 of the phthalide moiety of the isoderivatives in the same manner as in the TetR(D)/[MgCTC]$^+$ complex with distances of 3.6 Å (iso-CNTC) and 3.5 Å (iso-CTC). The former unfavorable contacts appear more suitable because hydroxyl O6 of CTC became an ester oxygen with decreased polarity.

Mg^{2+} Coordination. The crystal structure clearly shows that there is no metal chelation maintained by TetR(D) and iso-CTC, although Mg^{2+} ions were present in the crystallization setup of the iso-CTC complex. In TetR(D) complexes with [MgTc]$^+$ the oxygen atoms O11 and O12 are part of the β-ketoenolate moiety chelating the divalent metal ion, which is assumed to be mandatory for the mechanism of induction.[32] The octahedral coordination sphere is completed by Nε2 of His100 and three aqua ligands. In the iso-TCs O11 becomes part of the new lactone ring, and in both iso-TC complexes metal chelation is abolished. The position and distance of O12 to His100Nε2 are almost unchanged compared to the [MgCTC]$^+$ complex with 2.9 Å. The interaction of carbonyl O12 with His100Nε2 has to be assumed as hydrogen bond (Figure 3B) with distances of 3.1 and 3.0 Å in the cases of iso-CNTC and iso-CTC, respectively. Residue Thr103 is a key residue in the induction mechanism because its hydroxyl and carbonyl oxygen atoms stabilize the induced β-turn by hydrogen-bonding tow water ligands of the Mg^{2+} coordination sphere. Since the Mg^{2+} ion is missing, there is no direct link of the supposed inducing molecule to stabilize the induced β-turn (residues 100−103). This might be the major reason why TetR(D)/iso-TC complexes do not have or do not have unambiguously the induced conformation.

Allosteric Changes in TetR(D). Previous studies on the induction mechanism of TetR(D) showed that binding of a [MgTc]$^+$ complex to TetR(D) leads to a shift of helix α9′ ("sliding door") toward the tetracycline closing the binding tunnel.[33] We superimposed the not-induced structure of TetR(D)/iso-CNTC with the induced TetR(D)/[MgCTC]$^+$ complex (PDB code 2TCT) and the not-induced TetR(D) structure (PDB code 1A6I). Surprisingly, helix α9′ adopts the position of the induced TetR(D)/[MgCTC]$^+$ complex, although the TetR(D)/iso-CNTC complex is not-induced according to the α-helical rather than β-turn conformation of residues 100−103 (Figure 3C). The same result can be obtained upon superposition of TetR(D)/[MgCTC]$^+$ with the TetR(D)/iso-CTC complex, which has an uncertain status of induction. Therefore, the shift of α9′ is supported by hydrophobic interactions to the tetracycline ring D because C-terminal residues of α9 are mainly hydrophobic and in direct neighborhood to the D-ring. This shift may strengthen van der Waals interactions between side chains of α9′ and iso-CNTC (iso-CTC) as well as not degrade tetracyclines.

Affinity of Iso-CTC for TetR(D). Because of a low association constant and the resulting absorption effects at high protein and analyte concentrations when performing fluorescence titrations, binding of iso-CTC to TetR(D) was investigated by SPR. The binding of CTC to TetR(D) was also analyzed by SPR and compared with association constants measured by fluorescence kinetics because binding of CTC to TetR(D) results in strong fluorescence. In the absence of Mg^{2+} ions, association constants of CTC to TetR(D) were determined by SPR and fluorescence titrations with K_a = 2.36 ± 1.51 μM^{-1} and K_a = 2.30 ± 0.14 μM^{-1}, respectively. The results of the fluorescence and SPR measurements are the same within error bars. An association

dx.doi.org/10.1021/jm200332e |J. Med. Chem. 2011, 54, 5108–5115

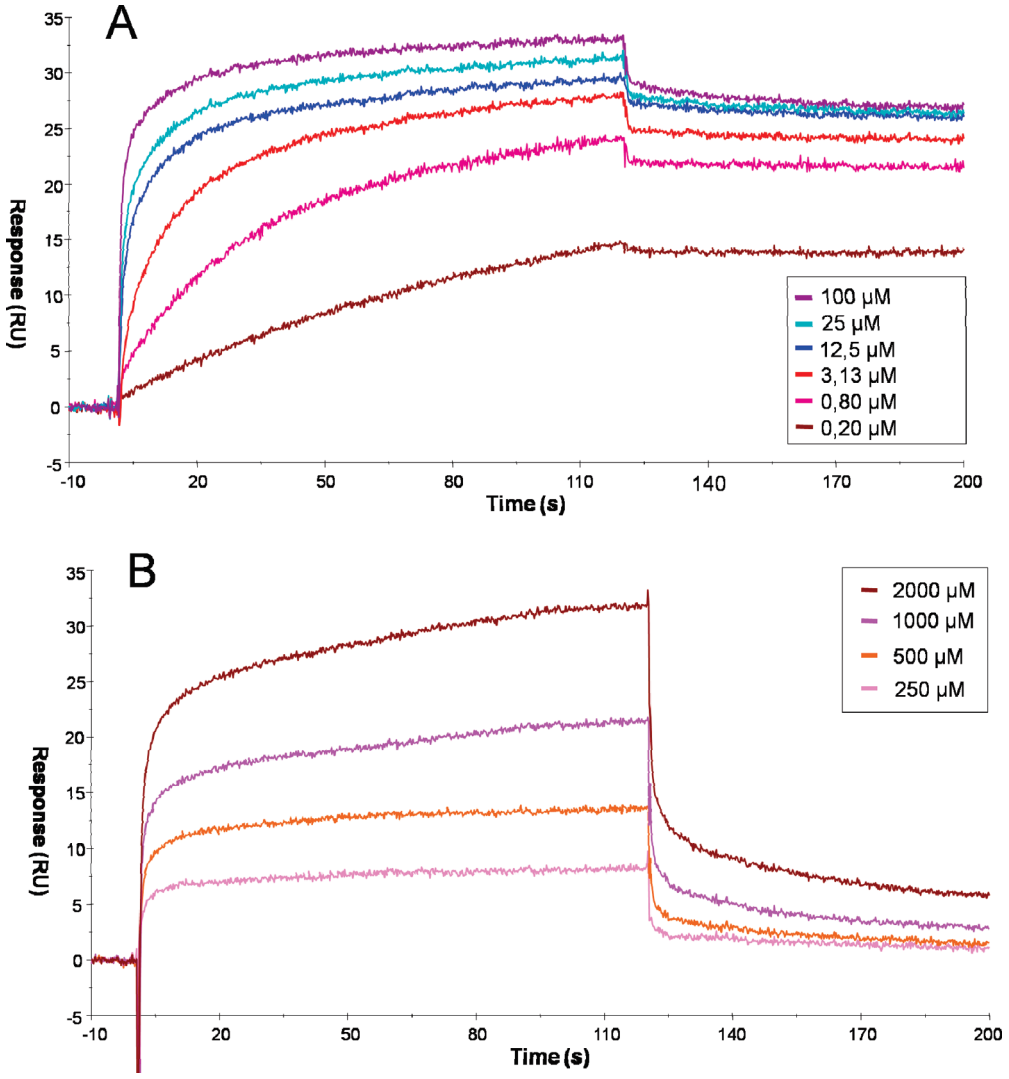

Figure 4. Binding of CTC and iso-CTC to immobilized TetR(D) as measured by surface plasmon resonance. Series S sensor chips CM5 were coated with TetR(D). CTC and iso-CTC were used as analytes. (A) Sensorgram of CTC binding to TetR(D). (B) Sensorgram of iso-CTC binding to TetR(D).

constant of $K_a = 0.80 \pm 0.49\ mM^{-1}$ was determined by SPR for iso-CTC binding to TetR(D). Thus, binding of iso-CTC to TetR(D) is detectable but about 3 orders of magnitude weaker compared to its precursor CTC without Mg^{2+} ions (Figure 4). Binding affinities of tetracyclines to TetR(D) in the presence of divalent metal ions are in the nanomolar range.[17]

CONCLUSIONS

Isoforms of tetracycline antibiotics such as iso-CNTC or iso-CTC bind to some extent in a comparable manner like non-degraded tetracyclines to TetR(D). Binding of iso-TCs does not lead to induction of TetR(D) most probably because chelation of divalent metal ions such as Mg^{2+} is abolished. The AB fragment of iso-TCs still binds in the same manner to TetR(D) just as the intact antibiotic. Thus, the preorganized protein combines lock-and-key behavior for regions close to the unchanged ligands amide, enolate, and ammonium groups. Hydrophobic interactions contribute to binding of the newly formed phthalide fragment (the former rings C, D).

Iso-TCs are not active as antibiotics, but they fit into tetracycline binding pockets. It is possible that they contribute to the development and distribution of antibiotic resistance or sensitivity.[26] They can mimic the structure of nondegraded tetracyclines by binding to a variety of other biopolymers.[34] Since iso-TCs are major degradation products in soil, animal tissue, and organs, they may also influence ribosomal activity. Though iso-TCs do not clearly induce TetR(D), binding to a variety of tetracycline binding pockets is conceivable and should be taken into account in consideration of tetracycline effects on the environment.

EXPERIMENTAL SECTION

Recombinant Protein Expression and Purification. Recombinant TetR(D) protein was expressed in *E. coli* RB791 with pWH610 vector construct. Ampicillin and chloramphenicol were added to Luria−Bertani medium with a final concentration of 100 and 30 $\mu g \cdot mL^{-1}$. Overexpression of TetR(D) protein was induced by isopropyl-β-D-thiogalactoside with a final concentration of 1 mM at an A_{600} of 0.5. Cells were harvested by centrifugation after incubation at 37 °C with shaking

for 3 h. The cell pellet was resuspended in 10 mL of cell lysis buffer (50 mM Tris, pH 8.0, 1 mM EDTA, 0.02% (w/v) NaN_3) and stored at −20 °C until protein purification.

The purification of TetR(D) was performed based on a modified protocol published by Ettner et al.[35] After cell lysis by two cycles of French press, the cell debris was removed by 1 h of centrifugation at 8000 rpm followed by filtration of the protein containing supernatant through a 0.22 μm PES membrane. TetR(D) was purified by cation-exchange chromatography (Poros 20 HS 10/50 Applied Biosystems) with cell lysis buffer containing a linear gradient between 10 mM NaCl and 1000 mM NaCl. An additional anion-exchange chromatography step (Poros 20 HQ 10/50) using the same buffers was added to purify TetR(D) to homogeneity. The purity of TetR(D) containing fractions was verified by SDS−PAGE. TetR(D) was concentrated on a Millipore Ultrafree PES membrane (MWCO 10000) to a final concentration of 17.3 mg·mL^{-1} and mixed with the same volume of 2 mM iso-CTC (in 50 mM Tris, 200 mM NaCl, and 0.02% (w/v) NaN_3) or 2 mM iso-CNTC (in 50 mM Tris, 200 mM NaCl, 50 mM EDTA, and 0.02% (w/v) NaN_3).

Protein Crystallization, X-ray Data Collection, and Model Refinement. TetR(D) crystals in complex with isotetracyclines were obtained in the tetragonal space group $I4_122$ isomorphous to various tetracycline complexes of TetR(D),[27,31] using the hanging drop vapor diffusion method at 293 K (Table 1). Crystals of TetR(D) in complex with iso-CTC grew from a mixture of 2 μL of protein solution with the same amount of reservoir solution (50 mM Tris, pH 8.0, 1.1 M $(NH_4)_2SO_4$, 100 mM NaCl, 10 mM $MgCl_2$). TetR(D) in complex with iso-CNTC crystallized in the same way with reservoir solution containing 50 mM Tris, pH 9.5, 750 mM $(NH_4)_2SO_4$, 70 mM NaCl, and 1 mM EDTA. The hanging drops were equilibrated against 500 μL of precipitation buffer.

Diffraction data were collected using synchrotron radiation at EMBL beamline X13 at the synchrotron source DESY (Hamburg) equipped with a MarCCD. Crystals were flash-frozen to 100 K after replacing the reservoir solution completely with paraffin oil. For processing, indexing, and scaling the programs DENZO and SCALEPACK[36] were used. Initial refinement of both structures was possible with the polypeptide of TetR(D) as a starting model (PDB code 2TRT,[27]) using REFMAC[37] as implemented in the CCP4 suite[38] and COOT for model building and electron-density inspection.[39] The iso-TC molecules were unambiguously identified at an early stage of refinement. After final model building and refinement omit electron density maps at the ligand-binding site were inspected. To avoid model bias, iso-TCs were excluded from the structure factor calculations and restrained refinement to convergence with REFMAC5 was carried out. FFT (CCP4 suite[38]) with the default settings for grid sampling was used to produce $2F_o - F_c$ and $F_o - F_c$ maps (Figure 2A). Molecular graphics images were prepared using the UCSF Chimera package[40] and PyMOL.[41] Superposition was carried out with the program SUPERPOSE (CCP4 suite) based on the rigid core of the TetR(D) dimer (helices α8, α10, α8′, α10′).

Surface Plasmon Resonance. For SPR measurements iso-CTC was obtained from a solution of CTC in 15% NaOH heated to 80 °C for 30 min. The solution was neutralized with HCl and loaded on a SOURCE 5RPC ST 4.6/150 column (GE Healthcare) equilibrated with pure water. Iso-CTC eluted with 22−25% acetonitrile, whereas CTC eluted with 36−39% acetonitrile. Fractions containing iso-CTC were lyophilized and stored in the dark at 4 °C until usage.

For SPR analysis, a BIAcore T100 machine equipped with a series S sensor chip CM5 and the amine coupling kit containing 1-ethyl-3-(3-dimethylaminopropyl)carbodiimide hydrochloride (EDC), *N*-hydroxysuccinimide (NHS), and ethanolamine−HCl, pH 8.5, were used (GE Healthcare). Protein immobilization was performed with HBS-EP+ (10 mM Hepes, pH 7.4, 150 mM NaCl, 0.05% (v/v) surfactant P20, 3 mM EDTA (GE Healthcare)) as running buffer at 10 μL/min. The four cells of the chip were activated with a mixture of EDC and NHS. Cells 2 and 4 were coated with 20 μg·mL^{-1} TetR(D) in 10 mM sodium acetate (pH 5.0) for 600 s, whereas cells 1 and 3 were kept as references. Free carboxymethyl groups were blocked by injecting 1 M ethanolamine−HCl, pH 8.5, on cells 1−4. Resulting SPR signals for immobilized TetR(D) on cells 2 and 4 were found to be 3740 and 5707 resonance units, respectively.

After chip equilibration with 150 mM NaCl, 50 mM Tris, pH 8, and 0.05% Tween 20, the interaction of TetR(D) with iso-CTC or CTC was measured at 298 K by injecting different concentrations of iso-CTC or CTC on cells 1 and 2 or cells 4 and 3, respectively, at a flow rate of 30 μL·min^{-1} for 120 s followed by a subsequent injection of running buffer for 300 s. Regeneration of the chip surface was performed with 1 mM glycine (pH 3.0) for 7 s. The association constant K_a for CTC and iso-CTC was determined using the affinity option in the BIA evaluation software package (GE Healthcare). Mean values and standard deviations were calculated for triplicate measurements.

Table 1. Data collection and refinement statistics[a]

	protein/isotetracycline complex	
	TetR(D)/iso-CTC PDB code 2X9D	TetR(D)/iso-CNTC PDB code 2X6O
Data Collection		
wavelength (Å)	0.9790	0.9790
resolution (Å)	63.76−2.34 (2.39−2.34)	27.43−2.30 (2.34−2.30)
tetragonal space group	$I4_122$	$I4_122$
unit cell parameter		
$a = b$; c (Å)	68.253; 179.27	69.050; 180.61
mosaicity (deg)	1.0	0.6
no. of measured reflections	40904	115247
no. of unique reflections	9121	10003
redundancy	4.48 (3.44)	11.45 (7.58)
$I/\sigma(I)$	9.7 (1.8)	41.3 (10.9)
completeness (%)	97.2 (75.6)	99.7 (99.6)
R_{merge} (%)	7.2 (64.3)	3.6 (26.4)
Wilson B factor (Å^2)	45.2	51.5
solvent content (%)	34.6	31.7
Refinement		
resolution limits (Å)	63.76−2.34	27.43−2.30
total reflections	9121	10003
no. of reflections in working set	8209	9007
no. of reflections in test set	912 (10%)	996 (10%)
R (%)	19.5	21.4
R_{free} (%)	25.2	26.9
figure of merit	0.81	0.75
no. of amino acid residues	207	207
no. of ligand/solvent molecules	1/68	1/50
rmsd bond lengths (Å)	0.012	0.018
rmsd bond angles (deg)	1.447	1.670
Ramachandran favored (%)	96.84	95.30

[a] Values in parentheses correspond to values in the highest resolution shell.

dx.doi.org/10.1021/jm200332e |*J. Med. Chem.* 2011, 54, 5108–5115

Fluorescence Measurements. For fluorescence measurements TetR(D) protein with a concentration of 1.5 μM was titrated with a 75 μM solution of CTC in a buffer composed of 150 mM NaCl, 50 mM Tris, pH 8, and 10 mM EDTA. Fluorescence was detected by a Safas Xenius model XC equipped with an automated titration device (SAFAS, Monaco) with excitation and emission wavelengths of 384 and 510 nm, respectively. The association constant K_a was determined according to Palm et al.[17]

Accession Codes

[†]The atomic coordinates of TetR(D) cocrystal complex structures have been made publicly available through the Protein Data Bank (www.rcsb.org/pdb) with the following PDB accession codes: isocyanotetracycline complex, 2X6O; isochlortetracycline complex, 2X9D.

AUTHOR INFORMATION

Corresponding Author

*Phone: (049) 3834 864356. Fax: (049) 3834 864373. E-mail: winfried.hinrichs@uni-greifswald.de.

ACKNOWLEDGMENT

Both iso-TC samples for crystallization were a gift from George A. Ellestad (Wyeth Ayerst Research, Pearl River, NY, U.S.). Helpful discussion with Gottfried J. Palm is acknowledged.

ABBREVIATIONS USED

TetR, Tet repressor; TetR(D), Tet repressor class D; Tc, tetracycline; iso-TC, isotetracycline; CNTC, 7-chlor-2-cyanotetracycline; CTC, 7-chlortetracycline (aureomycin); iso-CNTC, 6-iso-7-chlor-2-cyanotetracycline; iso-CTC, 6-iso-7-chlortetracycline; rmsd, root-mean-square deviation

REFERENCES

(1) Brodersen, D. E.; Clemons, W. M., Jr.; Carter, A. P.; Morgan-Warren, R. J.; Wimberly, B. T.; Ramakrishnan, V. The structural basis for the action of the antibiotics tetracycline, pactamycin, and hygromycin B on the 30S ribosomal subunit. *Cell* **2000**, *103* (7), 1143–1154.

(2) Heffron, S. E.; Mui, S.; Aorora, A.; Abel, K.; Bergmann, E.; Jurnak, F. Molecular complementarity between tetracycline and the GTPase active site of elongation factor Tu. *Acta Crystallogr. D* **2006**, *62* (Part 11), 1392–1400.

(3) Pioletti, M.; Schlünzen, F.; Harms, J.; Zarivach, R.; Gluhmann, M.; Avila, H.; Bashan, A.; Bartels, H.; Auerbach, T.; Jacobi, C.; Hartsch, T.; Yonath, A.; Franceschi, F. Crystal structures of complexes of the small ribosomal subunit with tetracycline, edeine and IF3. *EMBO J.* **2001**, *20* (8), 1829–1839.

(4) Saenger, W.; Orth, P.; Kisker, C.; Hillen, W.; Hinrichs, W. The tetracycline repressor: a paradigm for a biological switch. *Angew. Chem., Int. Ed.* **2000**, *39* (12), 2042–2052.

(5) Yamaguchi, A.; Udagawa, T.; Sawai, T. Transport of divalent cations with tetracycline as mediated by the transposon Tn10-encoded tetracycline resistance protein. *J. Biol. Chem.* **1990**, *265* (9), 4809–4813.

(6) Berens, C.; Lochner, S.; Lober, S.; Usai, I.; Schmidt, A.; Drueppel, L.; Hillen, W.; Gmeiner, P. Subtype selective tetracycline agonists and their application for a two-stage regulatory system. *ChemBioChem* **2006**, *7* (9), 1320–1324.

(7) Nelson, M.; Hillen, W.; Greenwald, R. A. *Tetracyclines in Biology, Chemistry and Medicine*; Birkhäuser Verlag: Basel, Switzerland, 2001.

(8) Volkers, G.; Palm, G. J.; Weiss, M. S.; Wright, G. D.; Hinrichs, W. Structural basis for a new tetracycline resistance mechanism relying on the TetX monooxygenase. *FEBS Lett.* **2011**, *585* (7), 1061–1066.

(9) Davies, A. K.; McKellar, J. F.; Phillips, G. O.; Reid, A. G. Photochemical oxidation of tetracycline in aqueous solution. *J. Chem. Soc., Perkin Trans. 2* **1979**, *1*, 369–375.

(10) Stephens, C. R.; Conover, L. H.; Gordon, P. N.; Pennington, F. C.; Wagner, R. L.; Brunings, K. J.; Pilgrim, F. J. Epitetracycline: the chemical relationship between tetracycline and quatrimycin. *J. Am. Chem. Soc.* **1956**, *78* (7), 1515–1516.

(11) Blanchflower, W. J.; McCracken, R. J.; Haggan, A. S.; Kennedy, D. G. Confirmatory assay for the determination of tetracycline, oxytetracycline, chlortetracycline and its isomers in muscle and kidney using liquid chromatography−mass spectrometry. *J. Chromatogr., B* **1997**, *692* (2), 351–360.

(12) Yuen, P. H.; Sokoloski, T. D. Kinetics of concomitant degradation of tetracycline to epitetracycline, anhydrotetracycline, and epianhydrotetracycline in acid phosphate solution. *J. Pharm. Sci.* **1977**, *66* (11), 1648–1650.

(13) McCormick, J. R.; Jensen, E. R.; Johnson, S.; Sjolander, N. O. Biosynthesis of the tetracyclines. IX. 4-Aminodedimethylaminoanhydrodemethylchlortetracycline from a mutant of *Streptomyces aureofaciens*. *J. Am. Chem. Soc.* **1968**, *90* (8), 2201–2202.

(14) Waller, C.; Hutchings, B.; Wolf, C.; Goldmann, A.; Broschard, R.; Williams, J. Degradation of aureomycin. VI. Isoaureomycin and aureomycin. *J. Am. Chem. Soc.* **1952**, *74*, 4981.

(15) Clive, D. L. J. Chemistry of tetracyclines. *Chem. Soc. Rev.* **1968**, *22*, 435–456.

(16) Soeborg, T.; Ingerslev, F.; Halling-Sorensen, B. Chemical stability of chlortetracycline and chlortetracycline degradation products and epimers in soil interstitial water. *Chemosphere* **2004**, *57* (10), 1515–1524.

(17) Palm, G. J.; Lederer, T.; Orth, P.; Saenger, W.; Takahashi, M.; Hillen, W.; Hinrichs, W. Specific binding of divalent metal ions to tetracycline and to the Tet repressor/tetracycline complex. *J. Biol. Inorg. Chem.* **2008**, *13* (7), 1097–1110.

(18) Dürkheimer, W. Tetracyclines: chemistry, biochemistry and structure−activity relations. *Angew. Chem., Int. Ed. Engl.* **1975**, *14* (11), 721–734.

(19) Nelson, M. L.; Park, B. H.; Levy, S. B. Molecular requirements for the inhibition of the tetracycline antiport protein and the effect of potent inhibitors on the growth of tetracycline-resistant bacteria. *J. Med. Chem.* **1994**, *37* (9), 1355–1361.

(20) Halling-Sorensen, B.; Sengelov, G.; Tjornelund, J. Toxicity of tetracyclines and tetracycline degradation products to environmentally relevant bacteria, including selected tetracycline-resistant bacteria. *Arch. Environ. Contam. Toxicol.* **2002**, *42* (3), 263–271.

(21) Arikan, O. A. Degradation and metabolization of chlortetracycline during the anaerobic digestion of manure from medicated calves. *J. Hazard. Mater.* **2008**, *158* (2−3), 485–490.

(22) Hamscher, G.; Sczesny, S.; Abu-Qare, A.; Höper, H.; Nau, H. Stoffe mit pharmakologischer Wirkung einschliesslich hormonell aktiver substanzen in der umwelt: nachweis von tetracyclinen in güllegedüngten böden. *DTW, Deutsch. Tieraerztl. Wochenschr.* **2000**, *107* (8), 332–334.

(23) Kennedy, D. G.; McCracken, R. J.; Hewitt, S. A.; McEvoy, J. D. Metabolism of chlortetracycline: drug accumulation and excretion in the hen's egg. *Analyst* **1998**, *123* (12), 2443–2447.

(24) Zurhelle, G.; Muller-Seitz, E.; Petz, M. Automated residue analysis of tetracyclines and their metabolites in whole egg, egg white, egg yolk and hen's plasma utilizing a modified ASTED system. *J. Chromatogr., B* **2000**, *739* (1), 191–203.

(25) Palmer, A. C.; Angelino, E.; Kishony, R. Chemical decay of an antibiotic inverts selection for resistance. *Nat. Chem. Biol.* **2010**, *6* (2), 105–107.

(26) Wright, G. D. Antibiotics: inactive but not inert. *Nat. Chem. Biol.* **2010**, *6* (2), 85–86.

(27) Hinrichs, W.; Kisker, C.; Düvel, M.; Muller, A.; Tovar, K.; Hillen, W.; Saenger, W. Structure of the Tet repressor−tetracycline complex and regulation of antibiotic resistance. *Science* **1994**, *264* (5157), 418–420.

(28) Orth, P.; Schnappinger, D.; Hillen, W.; Saenger, W.; Hinrichs, W. Structural basis of gene regulation by the tetracycline inducible Tet repressor−operator system. *Nat. Struct. Biol.* **2000**, *7* (3), 215–219.

(29) Aleksandrov, A.; Schuldt, L.; Hinrichs, W.; Simonson, T. Tet repressor induction by tetracycline: a molecular dynamics, continuum electrostatics, and crystallographic study. *J. Mol. Biol.* **2008**, *378* (4), 898–912.

(30) Kisker, C.; Hinrichs, W.; Tovar, K.; Hillen, W.; Saenger, W. The complex formed between Tet repressor and tetracycline−$Mg2^{+}$ reveals mechanism of antibiotic resistance. *J. Mol. Biol.* **1995**, *247* (2), 260–280.

(31) Aleksandrov, A.; Proft, J.; Hinrichs, W.; Simonson, T. Protonation patterns in tetracycline:tet repressor recognition: simulations and experiments. *ChemBioChem* **2007**, *8* (6), 675–685.

(32) Orth, P.; Saenger, W.; Hinrichs, W. Tetracycline-chelated Mg^{2+} ion initiates helix unwinding in Tet repressor induction. *Biochemistry* **1999**, *38* (1), 191–198.

(33) Orth, P.; Cordes, F.; Schnappinger, D.; Hillen, W.; Saenger, W.; Hinrichs, W. Conformational changes of the Tet repressor induced by tetracycline trapping. *J. Mol. Biol.* **1998**, *279* (2), 439–447.

(34) Dalm, D.; Palm, G. J.; Aleksandrov, A.; Simonson, T.; Hinrichs, W. Nonantibiotic properties of tetracyclines: structural basis for inhibition of secretory phospholipase A2. *J. Mol. Biol.* **2010**, *398* (1), 83–96.

(35) Ettner, N.; Müller, G.; Berens, C.; Backes, H.; Schnappinger, D.; Schreppel, T.; Pfleiderer, K.; Hillen, W. Fast large-scale purification of tetracycline repressor variants from overproducing *Escherichia coli* strains. *J. Chromatogr., A* **1996**, *742* (1−2), 95–105.

(36) Otwinowski, Z.; Minor, W. Processing of X-ray diffraction data collected in oscillation mode. *Methods Enzymol.* **1997**, *276*, 307–326.

(37) Murshudov, G. N.; Vagin, A. A.; Dodson, E. J. Refinement of macromolecular structures by the maximum-likelihood method. *Acta Crystallogr. D* **1997**, *53* (Part 3), 240–255.

(38) The CCP4 suite: programs for protein crystallography. *Acta Crystallogr. D* **1994**, *50*, (Part 5), 760−763.

(39) Emsley, P.; Cowtan, K. Coot: model-building tools for molecular graphics. *Acta Crystallogr. D* **2004**, *60* (12), 2126–2132.

(40) Pettersen, E. F.; Goddard, T. D.; Huang, C. C.; Couch, G. S.; Greenblatt, D. M.; Meng, E. C.; Ferrin, T. E. UCSF Chimera—a visualization system for exploratory research and analysis. *J. Comput. Chem.* **2004**, *25* (13), 1605–1612.

(41) Delano, W. L. *The PyMOL Molecular Graphics System*; DeLano Scientific: San Carlos, CA, 2002.